

1 **CDK11 is required for transcription of replication-dependent histone genes**

2

3 Pavla Gajdušková<sup>1,4</sup>, Igor Ruiz de Los Mozos<sup>2,3,4</sup>, Michal Rájecký<sup>1</sup>, Milan Hluchý<sup>1</sup>, Jernej  
4 Ule<sup>2,3</sup>, Dalibor Blazek<sup>1,5</sup>

5 <sup>1</sup>Central European Institute of Technology (CEITEC), Masaryk University, 62500 Brno,  
6 Czech Republic

7 <sup>2</sup>The Francis Crick Institute, Midland Rd, London, NW1 1AT, UK

8 <sup>3</sup>Department of Neuromuscular Disease, UCL Institute of Neurology, Queen Square, London,  
9 WC1N 3BG, UK

10 <sup>4</sup>These authors contributed equally to this publication

11 <sup>5</sup>Corresponding author

12 Contact: Dalibor Blazek, PhD. E-mail: dalibor.blazek@ceitec.muni.cz

13

14 **Abstract**

15 Replication-dependent histones (RDH) are required for packaging of newly synthesized DNA  
16 into nucleosomes during S-phase when their expression is highly upregulated. However, the  
17 mechanisms of this upregulation in metazoan cells remain poorly understood. Using iCLIP  
18 and ChIP-seq, we found that human cyclin-dependent kinase 11 (CDK11) associates with  
19 RNA and chromatin of RDH genes primarily in the S-phase. Moreover, its N-terminal region  
20 binds FLASH, RDH-specific 3' end processing factor, which keeps the kinase on the  
21 chromatin. CDK11 phosphorylates serine 2 (Ser2) of the C-terminal domain (CTD) of RNA  
22 polymerase II (RNAPII), which is initiated at the middle of RDH genes and is required for  
23 further RNAPII elongation and 3' end processing. CDK11 depletion leads to decreased  
24 number of cells in S-phase, likely due to the function of CDK11 in RDH gene expression.

25 Thus, the reliance of RDH expression on CDK11 could explain why CDK11 is essential for  
26 growth of many cancers.

27

28

29

30

31

32

33

34

35

36

37

38

39

40

41

42

43

44

45

46

47

48

49

50

51 **Introduction**

52 Transcription of protein-coding genes is mediated by RNA polymerase II (RNAPII) in  
53 several stages including initiation, elongation and termination <sup>1-3</sup>. RNAPII contains an  
54 unstructured C-terminal domain (CTD) with a series of evolutionarily conserved heptapeptide  
55 (YSPTSPS) repeats, where the individual serines (Ser), threonine (Thr), and tyrosine (Tyr)  
56 can each be phosphorylated to regulate various RNAPII functions <sup>4-6</sup>. Several kinases  
57 phosphorylate serine in position 2 (P-Ser2) <sup>6,7</sup>. This modification promotes RNAPII  
58 elongation and is necessary for coupling transcription with co-transcriptional processes, such  
59 as 3' end processing <sup>8-10</sup>.

60 Replication-dependent histone (RDH) proteins are required for packaging of newly  
61 synthesized DNA into nucleosomes before each cell division. Thus RDH genes have distinct  
62 regulation (and structure) from the rest of protein coding genes; they are expressed  
63 predominantly in S-phase and are short and intron-less. In humans there are approximately 80  
64 genes localized in 2 genomic clusters. Their transcripts are the only cellular non-  
65 polyadenylated mRNAs, carrying instead a conserved stem loop (SL) at their 3' end <sup>11</sup>.  
66 Expression of RDH genes is highly regulated by specific transcription and processing factors,  
67 including FLASH and SLBP proteins <sup>12</sup>. The ongoing transcription is linked with cascade  
68 recruitment of mRNA processing factors that form a platform to position the histone cleavage  
69 complex (HCC) at the 3' end of the RDH genes <sup>11</sup>. The HCC cleaves the pre-mRNA 5  
70 nucleotides after the SL, in a single processing step typical for the intron-less RDH  
71 transcripts <sup>13</sup>. Inefficient 3' end processing leads to transcriptional read-through and  
72 accumulation of small quantities of misprocessed and polyadenylated RDH transcripts (read-  
73 through RNAPII uses cryptic polyA sites) <sup>13,14</sup>. Notably, depletion of transcription elongation  
74 factors or slow elongation by mutant RNAPII results in production of small amounts of RDH

75 polyadenylated transcripts suggesting a link between transcriptional elongation and optimal  
76 3' end processing<sup>15-17</sup>.

77 As with other protein coding genes, the CTD of RNAPII participates in transcription  
78 and 3' end processing of RDH genes. Earlier studies suggested that CDK9-dependent P-Ser2  
79 and P-Thr4 regulate RDH-specific 3' end processing without affecting their transcription  
80<sup>15,18,19</sup>. However, genome-wide analyses of Thr4/Ala CTD mutants demonstrated that P-Thr4  
81 is needed for the global regulation of transcriptional elongation independently of CDK9<sup>20</sup>.  
82 Thus it remains unclear if or how any CTD-modifying enzyme (kinase) regulates RDH-  
83 specific transcription.

84 CDK11 (cyclin-dependent kinase 11) acts in complex with cyclins L1 and L2  
85 (CYCL1 and CYCL2)<sup>21</sup> and is expressed as two protein isoforms, CDK11<sup>p110</sup> and CDK11<sup>p58</sup>  
86<sup>22</sup>. CDK11<sup>p58</sup> is weakly expressed only in G2/M-phase of the cell cycle<sup>23,24</sup>. In contrast,  
87 abundantly and cell cycle-independently expressed CDK11<sup>p110</sup> differs from CDK11<sup>p58</sup> in the  
88 presence of 380 amino acid long N-terminal region which carries many charged amino acids  
89 and has an unknown function<sup>25</sup>. CDK11<sup>p110</sup> is ubiquitously expressed in all tissues and the  
90 CDK11<sup>p110</sup> null mouse is lethal at an early stage of development indicating an important role  
91 for CDK11<sup>p110</sup> in the adult as well as during development<sup>26</sup>. CDK11<sup>p110</sup> (from here on  
92 CDK11) is believed to play a role in RNAPII-directed transcription and co-transcriptional  
93 mRNA-processing<sup>27-29</sup>. However, its genome-wide function in regulating the human  
94 transcriptome is unknown. Notably, numerous recent studies identified CDK11 as a candidate  
95 essential gene for growth of several cancers<sup>30-35</sup>. Therefore, understanding the molecular  
96 mechanism(s) of CDK11-dependent gene expression would be of significant clinical interest.

97 In this study we find that CDK11 specifically regulates the expression of RDH genes.  
98 It binds to RDH RNAs and FLASH and associates with chromatin of RDH genes in a cell  
99 cycle-dependent manner. We further demonstrate that CDK11 can phosphorylate Ser2 in the

100 CTD of RNAPII positioned on the RDH genes to specifically control their transcriptional  
101 elongation and recruitment of 3' end processing factors.

102

## 103 **Results**

### 104 **CDK11 binds chromatin of RDH genes and promotes their transcription.**

105 To understand the role of CDK11 in human gene expression, we performed RNA-seq  
106 analyses from nuclear extracts of HCT116 cells treated with either control or CDK11 siRNA.  
107 CDK11 depletion resulted in down-regulation of 1131 genes ( $\log_2\text{FoldChange} < -1$ ,  $p$ -  
108  $\text{adj} < 0.01$ ) (**Fig. 1a, Supplementary Table 1**), with enrichment in gene ontology (GO) terms  
109 for nucleosome and chromatin organization (**Extended Data Fig. 1a, b**), indicating a role for  
110 CDK11 in regulating histone gene expression. Strikingly, 93% of expressed RDH genes (**Fig.**  
111 **1a**) were significantly downregulated (**Fig. 1b**), as confirmed by RT-qPCR for seven genes  
112 (**Extended Data Fig. 1c, d**). Nuclear run-on assays demonstrated a decrease in nascent  
113 mRNA of selected RDH genes in CDK11 knockdown cells (**Extended Data Fig. 1e**),  
114 indicating a transcriptional role of CDK11.

115 Next, we performed chromatin immunoprecipitation (ChIP-seq) to identify 393 peaks of  
116 CDK11 occupancy across the genome, which were enriched in GO terms for nucleosome and  
117 chromatin functions (**Extended Data Fig. 1f**). The peaks were present in 31 RDH genes, or  
118 71% of expressed RDH genes (see **Extended Data Fig. 1g**), but not in the remaining down-  
119 regulated genes (**Fig. 1c, Supplementary Table 2**). We confirmed specificity of signal with  
120 ChIP-qPCR on selected RDH genes from cells treated with control and CDK11 siRNAs  
121 (**Extended Data Fig. 1h**). These results indicate that CDK11 is recruited to the chromatin of  
122 RDH genes to **participate in** their transcription.

### 123 **FLASH recruits CDK11 to the RDH genes.**

124 To understand how CDK11 is specifically recruited to the chromatin of RDH genes,  
125 we tested whether CDK11 interacts with any known RDH-specific factors. For instance, the  
126 serine/threonine-rich FLASH protein associates only with the chromatin of RDH genes to  
127 regulate RDH-specific transcription and 3' end processing<sup>36,37</sup>. Notably, immunoprecipitation  
128 of endogenous FLASH resulted in a specific pulldown of CDK11 protein but not of CDK12<sup>38</sup>  
129 (**Fig. 2a**). Reciprocal immunoprecipitation of endogenous CDK11 from a cell line expressing  
130 flag-tagged FLASH (F-FLASH) showed an interaction between the proteins (**Extended Data**  
131 **Fig. 2a**), and F-FLASH also immunoprecipitated endogenous CDK11 (**Extended Data Fig.**  
132 **2b**), further confirming the result. To find whether interaction between FLASH and CDK11  
133 is direct, we expressed his-tagged fragments of FLASH (**Fig. 2b**) in *E. coli* and performed  
134 GST pulldown assay with GST-CDK11 purified from insect cells. The N- and C-terminal  
135 fragments of FLASH showed strong binding to CDK11, indicating the direct interaction  
136 between both proteins (**Fig. 2c**). Moreover, we found a strong overlap between the CDK11  
137 and FLASH<sup>36</sup> ChIP-seq occupancies solely on RDH genes (**Fig. 2d, Extended Data Fig. 2c**),  
138 indicating that the two proteins interact when present on chromatin. To test if CDK11  
139 recruitment depends on its interaction with FLASH we depleted FLASH from cells and  
140 measured CDK11 occupancy on RDH genes by ChIP-qPCR. This resulted in lower  
141 recruitment of CDK11 to the RDH genes (**Fig. 2e**) without affecting CDK11 protein levels  
142 (**Extended Data Fig. 2d**). Notably, the FLASH occupancy on the RDH genes was decreased  
143 comparably to the CDK11 occupancy (**Extended Data Fig. 2e**). Altogether, these results  
144 show that interaction with FLASH is needed for CDK11 recruitment to the RDH genes.

#### 145 **CDK11 is recruited to RDH genes predominantly in S-phase.**

146 Transcription of RDH genes occurs mostly in S-phase<sup>39</sup>. To understand if abundance and  
147 associations of FLASH and CDK11 with chromatin are cell cycle-dependent, we  
148 synchronized the cells by double thymidine treatment, which was confirmed by expression of

149 cell cycle markers (**Extended Data Fig. 3a**), RDH transcripts (**Extended Data Fig. 3b**) and  
150 by flow cytometry (**Extended Data Fig. 3c**). The abundance and phosphorylation of FLASH,  
151 as evident by its slower mobility on the gel (**Fig. 3a**), and its occupancy on RDH genes (**Fig.**  
152 **3b**) were highest in S-phase. Strikingly, CDK11 was required for the phosphorylation of  
153 FLASH in S-phase (**Fig. 3a, c, d**). In agreement, F-CDK11 can *in vitro* phosphorylate the N-  
154 terminal and central fragments of FLASH protein purified from bacteria (**Fig. 3e**). Notably,  
155 long treatments with CDK11 siRNA led to a strong decrease of FLASH protein levels  
156 (**Extended Data Fig. 3d**), whereas depletion of FLASH did not affect CDK11 protein levels  
157 (**Extended Data Fig. 3e**). Protein levels of CDK11 did not change during the cell cycle  
158 (**Extended Data Fig. 3a, Fig. 3a**), but it is enriched on RDH transcripts and chromatin in S-  
159 phase, as evident through F-CDK11 IP followed by RT-qPCR and ChIP-seq, respectively  
160 (**Fig. 3f, g**). For example, change is seen in *HIST1H4E* and *HIST1H1C* RDH genes  
161 (**Extended Data Fig. 3f**), but not on the control non-canonical histone *H3F3A* mRNA or on  
162 the non-RDH down-regulated genes identified from the RNA-seq experiment (**Fig. 3f, g**).  
163 Cell cycle analyses of CDK11-depleted cells manifested decreased numbers of cells in S- and  
164 their accumulation in G1-phase (**Fig. 3h**). The phenotype can result from deficient expression  
165 of RDH genes<sup>40</sup>. Collectively, our findings demonstrate that interaction with FLASH  
166 ensures that CDK11 is recruited to RDH genes specifically in S-phase, CDK11 also  
167 phosphorylates and maintains protein levels of FLASH and depletion of CDK11 leads to  
168 accumulation of cells in G1-phase at the expense of S-phase.

### 169 **RNA promotes CDK11 recruitment to the FLASH-containing RDH chromatin**

170 The N-terminal region (corresponding to amino acids 1-220) of human CDK11 is highly  
171 conserved, suggesting an important biological function (**Extended Data Fig. 4a**). It is rich in  
172 arginines and lysines, reminiscent of the intrinsically disordered regions that are common in  
173 non-canonical RNA-binding proteins<sup>41</sup> (**Fig. 4a**). Moreover, CDK11 was identified as a

174 candidate RNA-binding protein in two proteome-wide screens<sup>41,42</sup>. To examine the potential  
175 role of RNA binding in CDK11 functions, we performed individual-nucleotide resolution UV  
176 crosslinking and immunoprecipitation (iCLIP) (**Extended Data Fig. 4b**)<sup>43</sup> with an anti-Flag  
177 antibody from 293 cell lines stably expressing Flag-tagged CDK11 (F-CDK11), its N-  
178 terminal deletion mutant (F-CDK11<sub>226-783</sub>), or empty plasmid vector (F-EV) (**Extended Data**  
179 **Fig. 4b, c**). Two biological replicates of libraries crosslinked with 4-thiouridine (4SU) +  
180 365nm UV or 254nm were prepared from cells carrying F-CDK11 and F-CDK11<sub>226-783</sub>, with  
181 no-antibody or no-UV as negative controls (**Extended Data Fig. 4d, Supplementary Table**  
182 **3**). At least 5-15x more cDNAs were obtained from full length F-CDK11 compared to F-  
183 CDK11<sub>226-783</sub> (FDR<0.05) (**Supplementary Table 3**), indicating that RNA interaction is  
184 mediated primarily by the conserved N-terminal region. The unique cDNA counts of four  
185 replicates of F-CDK11 iCLIP revealed high correlation ( $R^2=0.64-0.84$ ) (**Extended Data Fig.**  
186 **4d**), and therefore we combined the replicates for further analyses. Largest proportion of  
187 binding was observed on noncoding RNAs (especially snRNAs) and 3' UTRs of mRNAs  
188 (**Extended Data Fig. 4e**).

189 We analysed the density of iCLIP significant crosslink sites (iCount, FDR < 0.05) in  
190 mRNAs, which identified 371 mRNAs with highest density (CLIP crosslink density > 0.01,  
191 **Supplementary Table 4**) enriched in GO terms for nucleosome and chromatin organization  
192 (**Extended Data Fig. 5a**). Notably, 30 RDH mRNAs were among the 100 most bound  
193 transcripts (**Supplementary Table 4**). A metaplot of summarised F-CDK11 crosslinking, and  
194 examples of *HIST1H3B* and *HIST1H1E* mRNAs, show that F-CDK11 binds primarily at the  
195 3'ends of RDH genes, just upstream of the conserved SL sequence (**Fig. 4b, c, Extended**  
196 **Data Fig. 5b**). Binding was strongly diminished in the F-CDK11<sub>226-783</sub> mutant and absent in  
197 the uncrosslinked F-CDK11. In contrast, other abundant protein-coding mRNAs, including  
198 cell cycle-independent non-canonical histones, either do not bind CDK11 or have much



199 weaker binding as compared to RNA-seq (**Extended Data Fig. 5c, d, e**), excluding scenario  
200 of false positive binding of highly expressed genes, such as RDH genes, in iCLIP assays <sup>44</sup>. A  
201 comparison of CDK11 iCLIP to eCLIP data from ~200 proteins in the ENCODE database <sup>44</sup>  
202 indicates that CDK11 likely binds nascent mRNAs, suggesting it interacts with RDH  
203 transcripts during transcription (data not shown). The specificity of CDK11 enrichment on  
204 RDH transcripts and the importance of the N-terminal region was further validated with UV-  
205 RNA immunoprecipitation (UV-RIP) followed by RT-qPCR, using F-CDK11<sub>226-783</sub>, CDK11  
206 knockdown, mock IP (no Ab) and the non-canonical histone *H3F3A* mRNA as controls  
207 (**Extended Data Fig. 5f-i**). We constructed myc-tagged variants to demonstrate that the  
208 residual association of F-CDK11<sub>226-783</sub> with RDH mRNA (**Extended Data Fig. 5h**) most  
209 likely results from its interaction with full length CDK11 (**Extended Data Fig. 5j**). We could  
210 not identify any strongly enriched unique sequence motif at CDK11-binding sites (data not  
211 shown), a situation common for non-canonical RNA-binding proteins.

212 To understand if RNA binding contributes to the association of CDK11 with chromatin, we  
213 performed subnuclear fractionation <sup>45</sup>, which was then either left untreated or incubated with  
214 RNases before further fractionating it into nucleoplasmic (soluble2) and chromatin (nuclear  
215 insoluble) fractions (**Extended Data Fig. 6a**). Optimal fractionation was verified by the  
216 presence of phosphorylated RNAPII and histone 3 (H3) only in the chromatin fractions (**Fig.**  
217 **4d**). CDK11 was found in both nuclear soluble (1&2) and chromatin fractions (**Fig. 4d**), in  
218 agreement with a previous study <sup>21</sup>. Importantly, RNase treatment disengaged CDK11 from  
219 the chromatin fraction, in contrast to the proteins CDK9 and FUS, which were disengaged  
220 from the soluble2 fraction (**Fig. 4d**) <sup>45</sup>. In agreement with the reliance of the CDK11-  
221 chromatin interaction on RNA (**Fig. 4d**), the interaction between CDK11 and FLASH was  
222 partly RNase-sensitive (**Extended Data Fig. 6b**) even though chromatin association of  
223 FLASH was not dependent on RNA (**Extended Data Fig. 6c**). In concordance, CDK11 binds

224 FLASH via its N-terminal RNA-binding region (**Extended Data Fig. 6d**). Moreover,  
225 RNAPII transcription inhibition with either Amanitin or Triptolide led to considerable  
226 dissociation of CDK11 from chromatin (**Fig. 4e**) without affecting CDK11 proteins levels  
227 (**Extended Data Fig. 6e**). Thus, both RNA and active transcription are essential to bring  
228 CDK11 to the FLASH-containing RDH chromatin.

### 229 **CDK11 promotes elongation of RDH genes.**

230 CDK11 can phosphorylate the CTD of RNAPII *in vitro*<sup>46</sup>, and Ser2 in the CTD during HIV  
231 transcription<sup>47</sup>. We used an *in vitro* kinase assay (*IVKA*) to verify that CDK11  
232 phosphorylates GST-CTD, albeit its activity was weaker compared to the canonical and well  
233 characterized CDK9<sup>48</sup> (**Fig. 5a**). Next, we used P-Ser2 and P-Ser5 phospho-specific  
234 antibodies to find that CDK11 phosphorylated both Ser2 and Ser5, whereas the negative  
235 controls F-EV and CDK11 kinase dead (CDK11 KD) led to no phosphorylation (**Fig. 5b**).  
236 CDK9 primarily phosphorylated Ser5, and CDK12 phosphorylated both Ser2 and Ser5,  
237 which agrees with expectations (**Fig. 5b**)<sup>49</sup>. **P-Ser2 is associated with elongating RNAPII<sup>4</sup>**  
238 **and P-Ser2 ChIP-seq signal accumulates at the 3' ends of all genes (**Extended Data Fig. 7a**),**  
239 **including RDH genes (**Fig. 5c**), resembling CDK11 iCLIP and ChIP-seq profiles on RDH**  
240 **genes (**Fig. 4c, Extended Data Fig. 1g**, respectively). CDK11 knockdown led to a collapse**  
241 **of the P-Ser2 signal on RDH genes (**Fig. 5c-e, Extended Data Fig. 7b, Supplementary****  
242 **Table 5), with a much lower (~30%) decrease on highly expressed genes, and little effect on**  
243 **all other genes (**Extended Data Fig. 7a**). Notably, P-Ser2 ChIP-seq signal starts**  
244 **accumulating close to the middle of RDH gene bodies (**Fig. 5c**), which coincides with the**  
245 **peak of CDK11 ChIP-seq signal (**Fig. 1c, 5d, f**), suggesting that a “transition” point in**  
246 **transcriptional elongation is located approximately in the middle of RDH genes (**Fig. 5c**).**  
247 **CDK11 depletion led to the decline in P-Ser2 occupancy (**Fig. 5c**) from this “transition” point**  
248 **onward (**Fig. 5c, d, f**) and to the decrease of RNAPII occupancy specifically on RDH genes**

249 **(Fig. 5g, Supplementary Table 6)**. However, the decrease in total RNAPII levels was  
250 smaller than in P-Ser2 levels **(Fig. 5c-e, Extended Data Fig. 7b, c)** and no significant  
251 changes were seen in P-Ser5 or P-Thr4 signal on selected RDH genes **(Extended Data Fig.**  
252 **7d-g)**<sup>18</sup>. This indicates that CDK11 is required primarily for the onset of Ser2  
253 phosphorylation at the “transition” point in RDH genes, which is essential for their  
254 productive elongation **(Fig. 5c)**.

### 255 **CDK11 promotes 3’end processing of RDH genes.**

256 Slow RNAPII elongation disrupts RDH mRNA processing<sup>17</sup> and Ser2-phosphorylated CTD  
257 serves as a binding platform for factors involved in 3’end formation and processing<sup>10</sup>.  
258 Indeed, following CDK11 depletion, the occupancy of CPSF100, a component of the HCC<sup>13</sup>,  
259 **(Fig. 6a)** decreased on all tested RDH genes to a similar extent as P-Ser2, and more than  
260 RNAPII **(Fig. 6a-e)**. We also observed an increase by a factor of 3-5 in read-through  
261 (uncleaved) RDH transcripts **(Fig. 6f, Extended Data Fig. 8a, b, Supplementary Table 7)**.  
262 No increase in read-through transcript was seen in non-RDH bound genes (*MYC*, *MAZ*) and  
263 one RDH gene *HIST1H1C*, which contains a cryptic polyA signal immediately downstream  
264 of the SL<sup>50</sup> that becomes increasingly used upon CDK11 knockdown **(Extended Data Fig.**  
265 **8b)**. This phenomenon of increased cryptic polyA use was additionally observed in  
266 *HIST1H2AC*, *HIST1H2BD* and *HIST1H4E* genes, and could be induced also by depletion or  
267 inhibition of CDK9<sup>15</sup>, CDK7<sup>51</sup>, ARS2<sup>52</sup> and SLBP<sup>53</sup>, which contribute to transcription and  
268 mRNA processing of RDH genes **(Extended Data Fig. 8c-g, Supplementary Table 7)**. The  
269 **small** changes in read-through and/or use of cryptic polyadenylation sites are thus a likely  
270 result of defective 3’end processing upon CDK11 knockdown. We conclude that the CDK11-  
271 dependent phosphorylation of Ser2 is required for efficient elongation and 3’ end processing  
272 of RDH genes.

273

274 **Discussion**

275 Our study reveals that CDK11 interacts with FLASH, a factor which has been known  
276 to be present only at RDH genes<sup>36</sup>. We show that FLASH promotes selective recruitment of  
277 CDK11 to RDH genes predominantly in the S-phase. CDK11 occupies coding regions of  
278 RDH genes; the binding is strongest at the “transition” point close to the middle of the RDH  
279 genes, where it coincides with accumulation of P-Ser2 (Fig. 5c, d), which in turn promotes  
280 efficient elongation and 3’end processing of RDH transcripts (summary of genome-wide  
281 data, working model and iCLIP- and ChIP-seq data on example RDH genes are presented in  
282 Fig. 7a, b and Extended Data Fig. 9a-f, respectively). CDK11 occupancy on RDH genes  
283 does not overlap with promoter-paused RNAPII (Fig. 1c, 5e) hence CDK11 likely does not  
284 mediate RNAPII transition to early elongation, the step regulated by CDK9 on most protein-  
285 coding genes<sup>48</sup>. CDK11 phosphorylates GST-CTD *in vitro*, but less efficiently than CDK9  
286 or CDK12 (Fig. 5a and data not shown), indicating that it might phosphorylate just a subset  
287 of CTD repeats, which could ensure an RDH-specific function of CDK11 in RNAPII-  
288 mediated transcription. CDK11 also phosphorylates FLASH, perhaps regulating FLASH  
289 stability however the exact *in vivo* function(s) of the phosphorylation(s) remains to be  
290 determined. We find that the arginine-rich N-terminus of CDK11 contacts RNA, we used  
291 iCLIP to identify its binding to RDH transcripts, particularly strong at their 3’ends, and we  
292 show that such RNA binding helps to maintain CDK11 on chromatin (Fig. 7a, b, Extended  
293 Data Fig. 9a-f).

294 CDK11 homolog is absent from yeast *Saccharomyces cerevisiae*, while the CDK11  
295 homolog in *Schizosaccharomyces pombe* contains only the kinase domain without the N-  
296 terminus<sup>54</sup>. CDK11 is an essential gene in metazoans<sup>26</sup>, but not in *S. pombe*<sup>54,55</sup>, possibly  
297 because yeast species transcribe RDH genes only in the S-phase, and all RDH mRNAs are  
298 polyadenylated<sup>56</sup>. Thus, the role of CDK11 in promoting S-phase specific RDH

299 transcriptional elongation and processing appears to have evolved only in metazoans. We  
300 conclude that the RNA binding capacity contributes to maintaining metazoan CDK11 close to  
301 chromatin, where it further achieves specificity for RDH genes through direct interactions  
302 with FLASH.

303 Downregulation of RDH mRNAs by knockdown of various RDH-specific  
304 transcription/3'end processing factors causes a disruption of cell cycle by accumulation of  
305 cells in either G1- or early S-phase (this study, **Fig. 3h** and <sup>12,40,57</sup>). Alternatively, the  
306 downregulation can be explained by the reduction of number of cells in S-phase (when RDH  
307 expression occurs). Although we cannot completely exclude a direct role of CDK11 in  
308 regulation of cell cycle progression, it's binding to RDH chromatin and nascent transcripts  
309 and interaction with FLASH strongly suggests direct and specific function in RDH  
310 transcription. CDK11-specific inhibitor (when available) will allow to determine whether the  
311 kinase also directly regulates cell cycle progression. As P-CTD-specific antibodies have  
312 limitations in recognition of the specific epitopes <sup>58</sup>, the inhibitor in combination with mass  
313 spectrometric analyses <sup>59</sup> can be also used for identification of any CDK11- or RDH-  
314 specific-P-CTD pattern.

315 Altogether, considering the fundamental role of RDH gene expression for cellular  
316 replication and proliferation, the mechanism identified in our study could underlie the  
317 essential role of CDK11 in many cancers <sup>25,32,33</sup>, and could serve as a framework for  
318 developing CDK11 inhibitors with therapeutic potential. **Indeed, when this paper was in  
319 revision, the first potent CDK11 inhibitor was reported, identified as the mischaracterized  
320 anticancer agent <sup>60</sup>.**

321

322

323 **Acknowledgements**

324

325 We thank all members of Blazek and Ule laboratories for discussions throughout the project  
326 and helpful comments on the manuscript. We also wish to thank Dr. Jasnovidova (Stefl lab)  
327 for the GST-CTD, Dr. Wouters for the HCT116 Flp-in cell line, Zuzana Slaba for preparation  
328 of His-FLASH constructs and proteins and Dr. Bartholomeeusen and Dr. Dettenhofer for  
329 comments on the manuscript. The work was supported by the following grants from: the  
330 Czech Science Foundation (“16-10930S”), the Masaryk University (“MUNI/E/0080/2017”),  
331 the CEITEC (Project ‘CEITEC-Central-European Institute of Technology’  
332 [CZ.1.05/1.1.00/02.0068]) to D.B. and the European Research Council (617837-Translate) to  
333 J.U. The Francis Crick Institute receives its core funding from Cancer Research UK  
334 (FC001002), the UK Medical Research Council (FC001002), and the Wellcome Trust  
335 (FC001002).

336

### 337 **Author contributions**

338

339 P.G. performed most experiments except for radioactive *IVKA*, some experiments in cell  
340 cycle synchronized cells (M.H.), nuclear run-on, RNase protection assay, GST-pulldown,  
341 FLASH ChIP-qPCR and *IVKA* with P-specific antibodies (M.R.) and CDK11 and P-Ser5  
342 ChIP-qPCR (D.B). I.R.dl.M. performed all bioinformatics analyses under supervision of J.U.  
343 and with some input from P.G. and D.B.. D.B. conceived the study, acquired funding and  
344 wrote the manuscript with support of P.G, I.R.dl.M. and J.U. All authors discussed the design  
345 of experiments, analysed the data and commented on the manuscript.

346

### 347 **Competing interests**

348

349 The authors declare no competing interests.

350

351 **Figure legends**

352 **Figure 1 CDK11 binds chromatin of RDH genes and promotes their transcription.**

353 **a**, RNA-seq analysis of HCT116 cells following siRNA-mediated CDK11 knockdown.

354 Down- and up-regulated genes ( $-1 > \log_2 \text{FoldChange} > 1$ ;  $p\text{-adj} < 0.01$ ) are shown in red and

355 blue, respectively. Symbols of 41 down-regulated RDH and 5 most up-regulated genes are

356 shown for  $n=3$  biologically independent experiments.

357 **b**, RNA-seq metaplots (top) and heatmaps (bottom) of the RDH genes in control (siCTRL)

358 and CDK11 (siCDK11) siRNA treated cells. TSS=transcription start site; SL=stem loop.

359 **c**, CDK11 ChIP-seq on RDH and 200 other down-regulated genes. CDK11 and input data are

360 from  $n=4$  and  $n=3$  biologically independent experiments, respectively. TSS=transcription

361 start site, SL/TES=stem loop/transcription end site.

362 **Figure 2 FLASH recruits CDK11 to the RDH genes.**

363 **a**, Western blot analyses of immunoprecipitates of endogenous FLASH from HCT116 cells.

364 The blots were probed with the indicated antibodies.

365 **b**, Depiction of human FLASH protein and four his-tagged deletion mutants expressed in

366 bacteria. Deletion mutants A and B have an overlapping region between amino acids 490-

367 571.

368 **c**, Western blot analyses of *in vitro* binding assays of GST-CDK11 purified from insect cells

369 and his-tagged FLASH (HIS-FLASH) deletion mutants expressed in bacteria and depicted in

370 Figure 2b.

371 **d**, FLASH ChIP-seq in hTERT cells (GSE69149)<sup>36</sup> (left panel) in comparison to CDK11

372 ChIP-seq (middle panel) and no Ab input control (right panel) on 44 regulated (expressed)

373 RDH (RDH with base mean expression  $> 10$ ), all RDH and 200 other downregulated genes.

374 **e**, Endogenous CDK11 ChIP-qPCR on indicated RDH genes or control intergenic region (Ir)  
375 in HCT116 cells treated either with control (CTRL) or FLASH siRNAs for 24 h. n=3  
376 biologically independent experiments, error bars=SEM, \*P<0.05, Student's two-sided t-test.  
377 Source Data for graphs in panel e are available with the paper on line.

378 **Figure 3 CDK11 is recruited to RDH genes predominantly in S-phase.**

379 **a**, Western blot analyses of extracts of HCT116 cells released from double thymidine  
380 synchronization. Time points after the release and cell cycle phases are indicated. Cell cycle  
381 phase markers: CCNA2=cyclin A2, SLBP. A=asynchronous cells, 0 h=time of the release.

382 **b**, FLASH ChIP-qPCR on selected RDH genes in asynchronous and G1/S, S and G2/M  
383 synchronised HCT116 cells. FLASH ChIP-qPCR signals are normalised to the maximum  
384 signal which was set as 1. n=3 biologically independent experiments, error bars=SEM,  
385 Ir=intergenic region.

386 **c**, Western blot analyses of FLASH and phosphorylated FLASH (P-FLASH) in cell lysates of  
387 HCT116 cells treated with either control or CDK11 or FLASH siRNAs for 48 h.

388 **d**, Western blot analyses of lysates of HCT116 cells synchronized by double thymidine  
389 treatment in G1/S-phase and released 2 h into the S-phase. The lysates were treated or were  
390 not with alkaline phosphatase (AP). The phosphorylated and dephosphorylated forms of  
391 FLASH and control RNAPII and Ser2 are indicated at right by clip marks and arrows,  
392 respectively. The blots were probed with indicated antibodies. P-FLASH, P-RNAPII and F-  
393 CDK11 are phosphorylated FLASH, RNAPII and Flag-tagged CDK11, respectively.

394 **e**, *IVKA* visualized by autoradiography (upper panel). His-tagged deletion mutants of FLASH  
395 expressed in bacteria were incubated with purified CDK11 in the presence of [ $\gamma$ -<sup>32</sup>P] ATP. P-  
396 FLASH=phosphorylated FLASH. Western blotting of inputs of FLASH deletion mutants  
397 (lower panel).



398 **f**, Graph displays RNA immunoprecipitation (RIP) of histone transcripts with F-CDK11 from  
399 HCT116 cells synchronized in G1/S-, S- and G2/M-phases. Graph shows fold change of  
400 CDK11 binding to RDH mRNA normalized to *MAZ* mRNA binding. mRNA levels in G1/S  
401 were set as 1 for each transcript. n=3 biologically independent experiments, error bars=SEM.

402 **g**, CDK11 ChIP-seq on the RDH and 200 other down-regulated genes in either HCT116 cells  
403 asynchronous or synchronized in S- or G2/M-phases. For asynchronous and S or G2/M n=4  
404 and 2 biologically independent experiments, respectively.

405 **h**, Histograms of cell cycle analyses of HCT116 cells transfected with control (CTRL) or  
406 CDK11 siRNA for 36 h. Percentage of cells in G0/G1-, S- and G2/M-phases are displayed.

407 Source data for panels b and f are available with the paper on line.

408 **Figure 4 RNA promotes CDK11 recruitment to the RDH chromatin.**

409 **a**, Schematic diagram highlighting the kinase domain and basic region of human CDK11  
410 protein.

411 **b**, Metagene analyses of F-CDK11 and F-CDK11 (226-783) iCLIP binding at all RDH  
412 transcripts from the TSS to the SL. iCLIP data k-means clustered, based on RNA-seq  
413 expression (high, medium and low). n=4 biologically independent experiments.

414 **c**, Biodalliance genome browser view of F-CDK11, F-CDK11 (226-783) and uncrosslinked  
415 control (no UV) iCLIP binding at *HIST1H3B* transcript. Stem loop (SL) is indicated by a  
416 black line.

417 **d**, Western blot analysis of association of the indicated factors in soluble and insoluble  
418 fractions of chromatin either treated or not treated with RNase A/T1. Arrows mark  
419 phosphorylated (upper) and non-phosphorylated (lower) forms of RNAPII. For CDK11, long  
420 and short exposures of the film are shown.

421 **e**, CDK11 ChIP-qPCR on RDH genes in HCT116 cells expressing stably integrated F-  
422 CDK11 and treated either with Amanitin (4 µg/ml) or Triptolide (10 µM) or untreated

423 (CTRL). n=4 biologically independent experiments, error bars=SEM, \*P<0.05, Student's t-  
424 test, Ir=intergenic region. Source data for panel e are available with the paper on line.

425 **Figure 5 CDK11 promotes transcriptional elongation of RDH genes.**

426 **a**, GST-CTD or BSA was incubated with the indicated cyclins/CDKs in the presence of [ $\gamma$ -  
427  $^{32}$ P] ATP, the resulting kinase reactions (*IVKA*) were resolved on SDS-PAGE gel and  
428 visualized by autoradiography. Phosphorylated GST-CTD (P-GST-CTD) and  
429 autophosphorylated CDK11 is shown (upper panel). Equal input of flag-tagged cyclins/CDKs  
430 and GST-CTD to the *IVKA* were confirmed by western blotting with anti-flag antibody  
431 (middle panel) or by Coomassie staining (lower panel), respectively.

432 **b**, Displayed cyclins/CDKs purified from HCT116 cells were incubated with GST-CTD in  
433 *IVKA*. Phosphorylation was monitored by the indicated antibodies by Western blotting (upper  
434 panel). Input of equal amounts of flag-tagged CDKs into *IVKA* was validated by flag  
435 antibody (lower panel). F=flag tag, X=express tag, KD=kinase dead mutant, end=endogenous,  
436 EV=empty vector.

437 **c**, ChIP-seq analyses of RNAPII and P-Ser2 occupancies on expressed RDH genes in  
438 HCT116 cells treated with either control (CTRL) or CDK11 siRNA. Transcription elongation  
439 “transition” point is indicated by dashed line. n=3 biologically independent experiments.

440 **d**, P-Ser2/RNAPII normalized ChIP-seq log<sub>2</sub> fold change on RDH genes after CDK11  
441 knockdown within differential P-Ser2 MACS2 peaks (depicted as P-Ser2 start (vertical  
442 dashed line) and P-Ser2 end).

443 **e**, *HIST1H4E* gene tracks with raw RNAPII and P-Ser2 ChIP-seq data and RNAPII, P-Ser2  
444 and P-Ser2/RNAPII log<sub>2</sub> fold change after CDK11 depletion. Black line indicates differential  
445 peaks identified by MACS2 program (p<0.05).

446 **f**, CDK11 ChIP-seq occupancy is most abundant just upstream of the differential P-Ser2  
447 MACS2 peaks in RDH genes. The start of the P-Ser2 peaks is indicated by vertical dashed  
448 line (see also Fig. 5d for metaplot and heatmap).

449 **g**, Violin-plots measure RNAPII occupancy on the TSS (top panel, flank 500 nt) and SL or  
450 TES (bottom panel, 250 nt upstream and 750 nt downstream) of expressed RDH and 200  
451 highly expressed and randomized genes.

452 **Figure 6 Recruitment of 3' end processing factor CPSF100 to the RDH genes depends**  
453 **on CDK11-mediated phosphorylation of Ser2.**

454 **a, b, c**, Graphs present ChIP-qPCR data for CPSF100 (a), RNAPII (b) and P-Ser2 (c) in  
455 HCT116 cells transfected with control (siCTRL) or CDK11 (siCDK11) siRNA. qPCR  
456 primers were designed in coding regions of RDH genes. n=4, n=3 and n=3 biologically  
457 independent experiments for (a), (b) and (c), respectively; error bars=SEM, Ir = intergenic  
458 region.

459 **d, e**. Graphs present ratios of CPSF100/RNAPII (d) and CPSF100/P-Ser2 (e) ChIP-qPCR  
460 signals. n=4 and 3 biologically independent experiments for (d) and (e), respectively; error  
461 bars=SEM, \*P<0.05, Student's two-sided t-test.

462 **f**, Subtracted RNA-seq (siCDK11 - siCTRL) RPKM normalized downstream of the SL until  
463 the next conserved polyadenylation site (33 RDH genes; distance from 27 nt to 15 kb) (upper  
464 panel). The read-through is depicted for indicated individual RDH genes carrying cryptic  
465 polyadenylation site downstream of SL (lower panel).

466 [Source data for panels a-e are available with the paper on line.](#)

467 **Figure 7 Summary of iCLIP and ChIP-seq data and working model.**

468 **a**, Each column in the table depicts distribution of iCLIP and ChIP-seq peaks over selected  
469 genes either affected or not in CDK11 RNA-seq (Fig. 1a). See Online Methods for further  
470 description. iCLIP peaks density of significant cross links cDNA normalized by gene length

471 (sig. > 0.01). CDK11 ChIP-seq bound RPGS inside MACS2 significant peak ( $p < 0.05$ ) to  
472 selected genes (sig. > 0.01). RNA-seq DE-Seq2 differentially expressed genes ( $-$   
473  $1 > \log_2 \text{FoldChange} > 1$ ,  $p\text{-adj} < 0.05$ ). P-Ser2 ChIP-seq RPGC siCDK11  $\log_2$  fold change  
474 inside the MACS2 differential expressed peaks ( $-1 > \log_2 \text{FoldChange} > 1$ ,  $p\text{-adj} < 0.05$ ,  
475 supplementary table 5). RNAPII ChIP-seq RPGC siCDK11  $\log_2$  fold change inside the  
476 differentially expressed peaks ( $-1 > \log_2 \text{FoldChange} > 1$ ,  $p\text{-adj} < 0.05$ , supplementary table 6).  
477 P-Ser2/RNAPII normalised ChIP RPGC siCDK11  $\log_2$  fold change inside the differential  
478 expressed peaks ( $-1 > \log_2 \text{FoldChange} > 1$ ,  $p\text{-adj} < 0.05$ , supplementary table 6). The groups of  
479 genes: 44 regulated RDH (base mean expression  $> 10$ ); 39 low- and non-expressed RDH (base  
480 mean expression  $< 10$ ); 10 most down- and up-regulated genes in CDK11 RNA-seq (in fuchsia  
481 and blue, respectively), 10 selected cell cycle-related genes (in green). All genes were sorted  
482 by base mean expression within each group. Gene symbols are shown on the right.

483 **b**, Schematic working model. CDK11 regulates transcription elongation of RDH genes and  
484 contributes to their 3' end processing. FLASH (grey flash) recruits CDK11 (red oval)  
485 collaboratively with nascent RDH mRNAs (black line) to chromatin of RDH genes (grey  
486 double helix) and phosphorylates (arrow) Ser2 (red ball) in the CTD (red and grey balls) of  
487 RNAPII (violet oval). The Ser2 phosphorylation promotes the RNAPII elongation on RDH  
488 genes. CDK11 also phosphorylates FLASH in S-phase which may be needed for its stability  
489 and/or yet unknown function in transcription/3' end processing of RDH genes. CDK11 is  
490 bound abundantly at the 3' end of RDH mRNAs and this binding likely occurs on or in the  
491 close vicinity of RDH chromatin. CDK11-dependent phosphorylation of Ser2 contributes to  
492 the recruitment of 3' end processing HCC complex (SYMPLEKIN (blue oval), CPSF100  
493 (green circle), CstF64 (brown circle) and CPSF73 (yellow circle) allowing CPSF73 to cleave  
494 nascent RDH mRNA (black line). FLASH interaction with U7 snRNP (white/blue circular  
495 complex) also contributes to the recruitment of the HCC to pre-mRNA<sup>11</sup>.

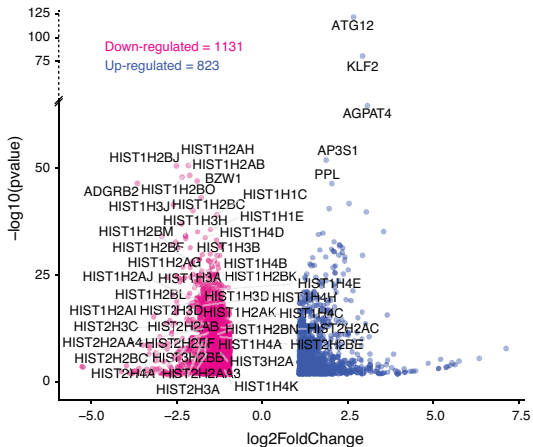
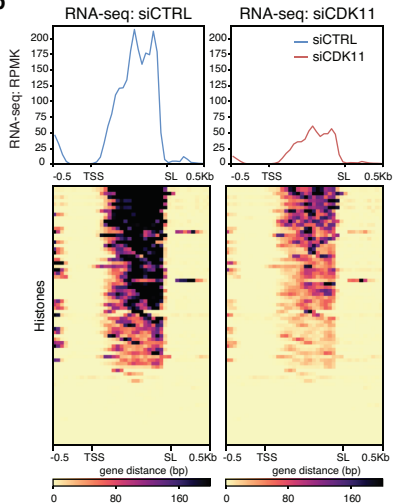
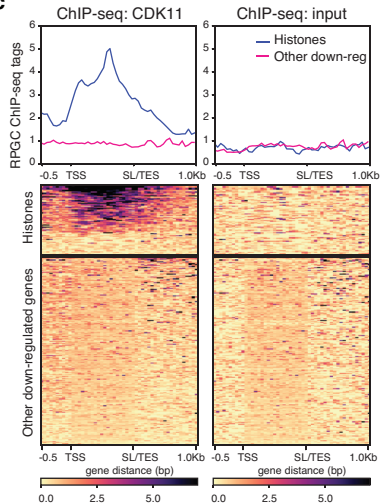
496 **References**

497

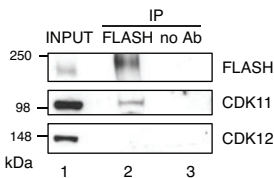
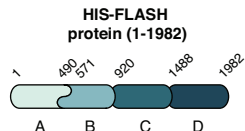
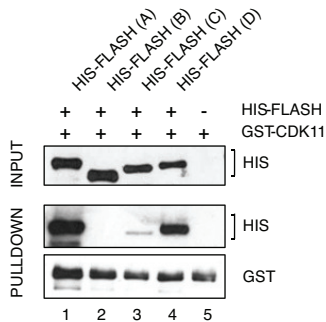
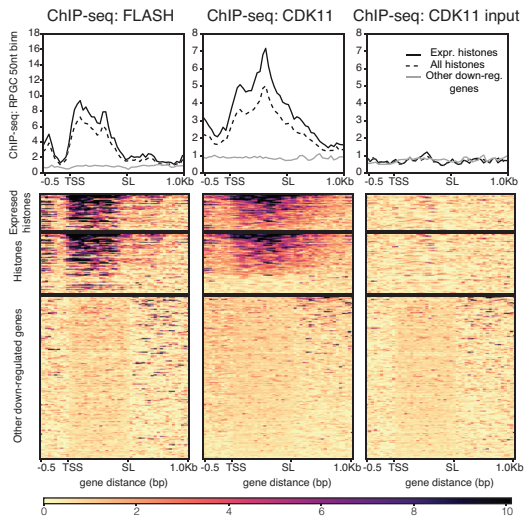
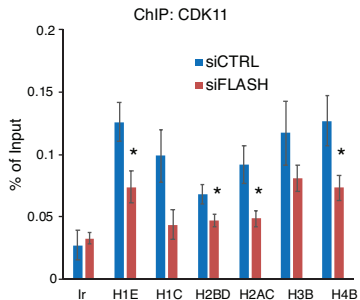
- 498 1. Adelman, K. & Lis, J.T. Promoter-proximal pausing of RNA polymerase II: emerging  
499 roles in metazoans. *Nat Rev Genet* **13**, 720-31 (2012).
- 500 2. Fuda, N.J., Ardehali, M.B. & Lis, J.T. Defining mechanisms that regulate RNA  
501 polymerase II transcription in vivo. *Nature* **461**, 186-92 (2009).
- 502 3. Proudfoot, N.J. Transcriptional termination in mammals: Stopping the RNA  
503 polymerase II juggernaut. *Science* **352**, aad9926 (2016).
- 504 4. Eick, D. & Geyer, M. The RNA polymerase II carboxy-terminal domain (CTD) code.  
505 *Chem Rev* **113**, 8456-90 (2013).
- 506 5. Harlen, K.M. & Churchman, L.S. The code and beyond: transcription regulation by  
507 the RNA polymerase II carboxy-terminal domain. *Nat Rev Mol Cell Biol* **18**, 263-273  
508 (2017).
- 509 6. Zaborowska, J., Egloff, S. & Murphy, S. The pol II CTD: new twists in the tail. *Nat*  
510 *Struct Mol Biol* **23**, 771-7 (2016).
- 511 7. Jeronimo, C., Collin, P. & Robert, F. The RNA Polymerase II CTD: The Increasing  
512 Complexity of a Low-Complexity Protein Domain. *J Mol Biol* **428**, 2607-2622  
513 (2016).
- 514 8. Bentley, D.L. Coupling mRNA processing with transcription in time and space. *Nat*  
515 *Rev Genet* **15**, 163-75 (2014).
- 516 9. Hsin, J.P. & Manley, J.L. The RNA polymerase II CTD coordinates transcription and  
517 RNA processing. *Genes Dev* **26**, 2119-37 (2012).
- 518 10. Herzelt, L., Ottoz, D.S.M., Alpert, T. & Neugebauer, K.M. Splicing and transcription  
519 touch base: co-transcriptional spliceosome assembly and function. *Nat Rev Mol Cell*  
520 *Biol* **18**, 637-650 (2017).
- 521 11. Marzluff, W.F. & Koreski, K.P. Birth and Death of Histone mRNAs. *Trends Genet*  
522 **33**, 745-759 (2017).
- 523 12. Duronio, R.J. & Marzluff, W.F. Coordinating cell cycle-regulated histone gene  
524 expression through assembly and function of the Histone Locus Body. *RNA Biol* **14**,  
525 726-738 (2017).
- 526 13. Sullivan, K.D., Steiniger, M. & Marzluff, W.F. A core complex of CPSF73,  
527 CPSF100, and Symplekin may form two different cleavage factors for processing of  
528 poly(A) and histone mRNAs. *Mol Cell* **34**, 322-32 (2009).
- 529 14. Kohn, M., Ihling, C., Sinz, A., Krohn, K. & Huttelmaier, S. The Y3\*\* ncRNA  
530 promotes the 3' end processing of histone mRNAs. *Genes Dev* **29**, 1998-2003 (2015).
- 531 15. Pirngruber, J. et al. CDK9 directs H2B monoubiquitination and controls replication-  
532 dependent histone mRNA 3'-end processing. *EMBO Rep* **10**, 894-900 (2009).
- 533 16. Narita, T. et al. NELF interacts with CBC and participates in 3' end processing of  
534 replication-dependent histone mRNAs. *Mol Cell* **26**, 349-65 (2007).
- 535 17. Saldi, T., Fong, N. & Bentley, D.L. Transcription elongation rate affects nascent  
536 histone pre-mRNA folding and 3' end processing. *Genes Dev* **32**, 297-308 (2018).
- 537 18. Hsin, J.P., Sheth, A. & Manley, J.L. RNAP II CTD phosphorylated on threonine-4 is  
538 required for histone mRNA 3' end processing. *Science* **334**, 683-6 (2011).
- 539 19. Medlin, J. et al. P-TEFb is not an essential elongation factor for the intronless human  
540 U2 snRNA and histone H2b genes. *EMBO J* **24**, 4154-65 (2005).
- 541 20. Hintermair, C. et al. Threonine-4 of mammalian RNA polymerase II CTD is targeted  
542 by Polo-like kinase 3 and required for transcriptional elongation. *EMBO J* **31**, 2784-  
543 97 (2012).

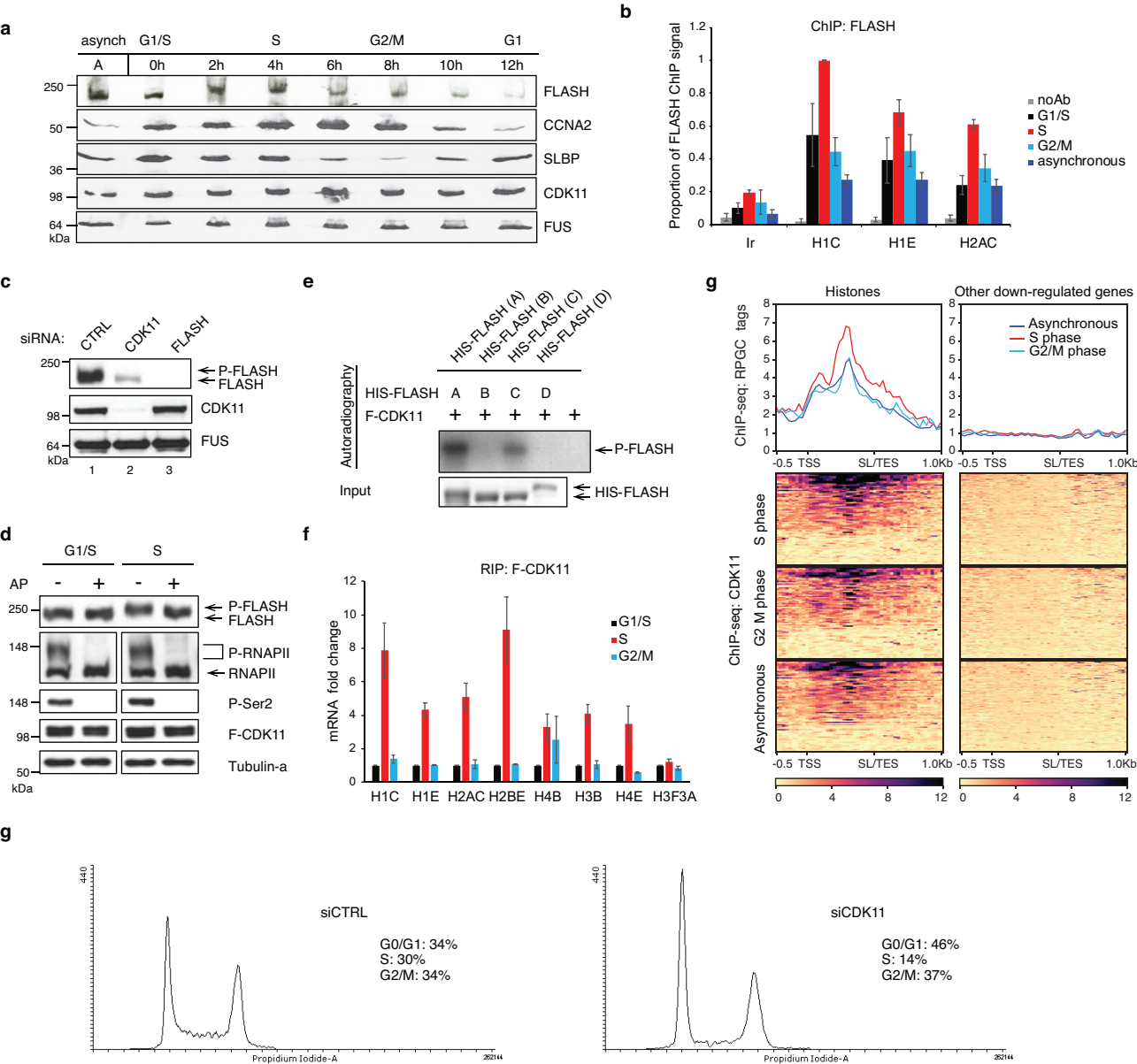
- 544 21. Loyer, P. et al. Characterization of cyclin L1 and L2 interactions with CDK11 and  
545 splicing factors: influence of cyclin L isoforms on splice site selection. *J Biol Chem*  
546 **283**, 7721-32 (2008).
- 547 22. Cornelis, S. et al. Identification and characterization of a novel cell cycle-regulated  
548 internal ribosome entry site. *Mol Cell* **5**, 597-605 (2000).
- 549 23. Hu, D., Valentine, M., Kidd, V.J. & Lahti, J.M. CDK11(p58) is required for the  
550 maintenance of sister chromatid cohesion. *J Cell Sci* **120**, 2424-34 (2007).
- 551 24. Petretti, C. et al. The PITSLRE/CDK11p58 protein kinase promotes centrosome  
552 maturation and bipolar spindle formation. *EMBO Rep* **7**, 418-24 (2006).
- 553 25. Zhou, Y., Shen, J.K., Hornicek, F.J., Kan, Q. & Duan, Z. The emerging roles and  
554 therapeutic potential of cyclin-dependent kinase 11 (CDK11) in human cancer.  
555 *Oncotarget* **7**, 40846-40859 (2016).
- 556 26. Li, T., Inoue, A., Lahti, J.M. & Kidd, V.J. Failure to proliferate and mitotic arrest of  
557 CDK11(p110/p58)-null mutant mice at the blastocyst stage of embryonic cell  
558 development. *Mol Cell Biol* **24**, 3188-97 (2004).
- 559 27. Hu, D., Mayeda, A., Trembley, J.H., Lahti, J.M. & Kidd, V.J. CDK11 complexes  
560 promote pre-mRNA splicing. *J Biol Chem* **278**, 8623-9 (2003).
- 561 28. Trembley, J.H. et al. PITSLRE p110 protein kinases associate with transcription  
562 complexes and affect their activity. *J Biol Chem* **277**, 2589-96 (2002).
- 563 29. Valente, S.T., Gilmartin, G.M., Venkatarama, K., Arriagada, G. & Goff, S.P. HIV-1  
564 mRNA 3' end processing is distinctively regulated by eIF3f, CDK11, and splice factor  
565 9G8. *Mol Cell* **36**, 279-89 (2009).
- 566 30. Tiedemann, R.E. et al. Identification of molecular vulnerabilities in human multiple  
567 myeloma cells by RNA interference lethality screening of the druggable genome.  
568 *Cancer Res* **72**, 757-68 (2012).
- 569 31. Chi, Y. et al. Abnormal expression of CDK11p58 in prostate cancer. *Cancer Cell Int*  
570 **14**, 2 (2014).
- 571 32. Duan, Z. et al. Systematic kinome shRNA screening identifies CDK11 (PITSLRE)  
572 kinase expression is critical for osteosarcoma cell growth and proliferation. *Clin*  
573 *Cancer Res* **18**, 4580-8 (2012).
- 574 33. Kren, B.T. et al. Preclinical evaluation of cyclin dependent kinase 11 and casein  
575 kinase 2 survival kinases as RNA interference targets for triple negative breast cancer  
576 therapy. *Breast Cancer Res* **17**, 524 (2015).
- 577 34. Liu, X. et al. Cyclin-Dependent Kinase 11 (CDK11) Is Required for Ovarian Cancer  
578 Cell Growth In Vitro and In Vivo, and Its Inhibition Causes Apoptosis and Sensitizes  
579 Cells to Paclitaxel. *Mol Cancer Ther* **15**, 1691-701 (2016).
- 580 35. Du, Y. et al. CDK11(p110) plays a critical role in the tumorigenicity of esophageal  
581 squamous cell carcinoma cells and is a potential drug target. *Cell Cycle* **18**, 452-466  
582 (2019).
- 583 36. Sokolova, M. et al. Genome-wide screen of cell-cycle regulators in normal and tumor  
584 cells identifies a differential response to nucleosome depletion. *Cell Cycle* **16**, 189-  
585 199 (2017).
- 586 37. Yang, X.C., Burch, B.D., Yan, Y., Marzluff, W.F. & Dominski, Z. FLASH, a  
587 proapoptotic protein involved in activation of caspase-8, is essential for 3' end  
588 processing of histone pre-mRNAs. *Mol Cell* **36**, 267-78 (2009).
- 589 38. Kohoutek, J. & Blazek, D. Cyclin K goes with Cdk12 and Cdk13. *Cell Div* **7**, 12  
590 (2012).
- 591 39. Marzluff, W.F., Wagner, E.J. & Duronio, R.J. Metabolism and regulation of canonical  
592 histone mRNAs: life without a poly(A) tail. *Nat Rev Genet* **9**, 843-54 (2008).

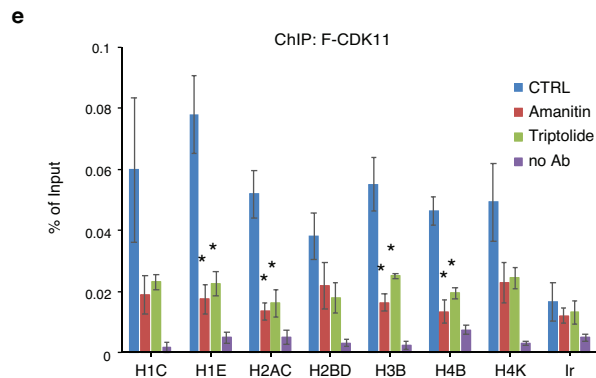
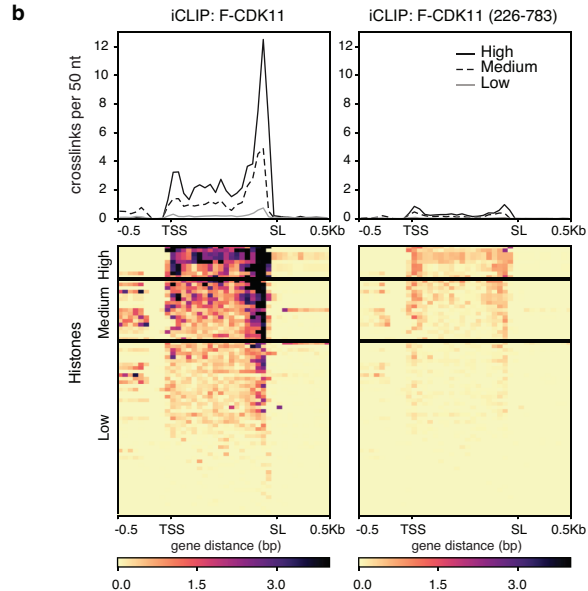
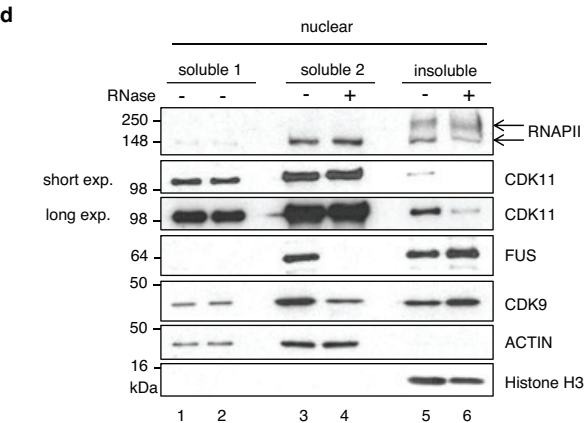
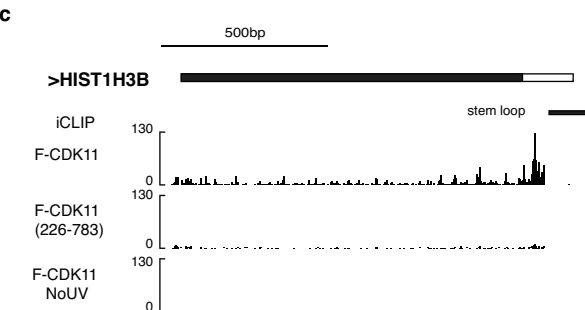
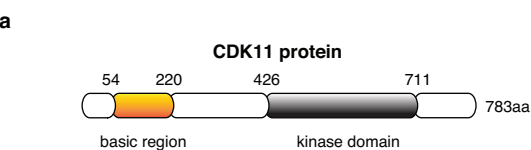
- 593 40. Zhao, J. et al. NPAT links cyclin E-Cdk2 to the regulation of replication-dependent  
594 histone gene transcription. *Genes Dev* **14**, 2283-97 (2000).
- 595 41. Castello, A. et al. Insights into RNA biology from an atlas of mammalian mRNA-  
596 binding proteins. *Cell* **149**, 1393-406 (2012).
- 597 42. Baltz, A.G. et al. The mRNA-bound proteome and its global occupancy profile on  
598 protein-coding transcripts. *Mol Cell* **46**, 674-90 (2012).
- 599 43. Konig, J. et al. iCLIP reveals the function of hnRNP particles in splicing at individual  
600 nucleotide resolution. *Nat Struct Mol Biol* **17**, 909-15 (2010).
- 601 44. Van Nostrand, E.L. et al. Robust transcriptome-wide discovery of RNA-binding  
602 protein binding sites with enhanced CLIP (eCLIP). *Nat Methods* **13**, 508-14 (2016).
- 603 45. Beltran, M. et al. The interaction of PRC2 with RNA or chromatin is mutually  
604 antagonistic. *Genome Res* **26**, 896-907 (2016).
- 605 46. Trembley, J.H., Hu, D., Slaughter, C.A., Lahti, J.M. & Kidd, V.J. Casein kinase 2  
606 interacts with cyclin-dependent kinase 11 (CDK11) in vivo and phosphorylates both  
607 the RNA polymerase II carboxyl-terminal domain and CDK11 in vitro. *J Biol Chem*  
608 **278**, 2265-70 (2003).
- 609 47. Pak, V. et al. CDK11 in TREX/THOC Regulates HIV mRNA 3' End Processing. *Cell*  
610 *Host Microbe* **18**, 560-70 (2015).
- 611 48. Peterlin, B.M. & Price, D.H. Controlling the elongation phase of transcription with P-  
612 TEFb. *Mol Cell* **23**, 297-305 (2006).
- 613 49. Bosken, C.A. et al. The structure and substrate specificity of human Cdk12/Cyclin K.  
614 *Nat Commun* **5**, 3505 (2014).
- 615 50. Lyons, S.M. et al. A subset of replication-dependent histone mRNAs are expressed as  
616 polyadenylated RNAs in terminally differentiated tissues. *Nucleic Acids Res* **44**, 9190-  
617 9205 (2016).
- 618 51. Larochelle, S. et al. Cyclin-dependent kinase control of the initiation-to-elongation  
619 switch of RNA polymerase II. *Nat Struct Mol Biol* **19**, 1108-15 (2012).
- 620 52. Gruber, J.J. et al. Ars2 promotes proper replication-dependent histone mRNA 3' end  
621 formation. *Mol Cell* **45**, 87-98 (2012).
- 622 53. Sullivan, K.D., Mullen, T.E., Marzluff, W.F. & Wagner, E.J. Knockdown of SLBP  
623 results in nuclear retention of histone mRNA. *RNA* **15**, 459-72 (2009).
- 624 54. Drogat, J. et al. Cdk11-cyclinL controls the assembly of the RNA polymerase II  
625 mediator complex. *Cell Rep* **2**, 1068-76 (2012).
- 626 55. Kim, D.U. et al. Analysis of a genome-wide set of gene deletions in the fission yeast  
627 *Schizosaccharomyces pombe*. *Nat Biotechnol* **28**, 617-623 (2010).
- 628 56. Kurat, C.F. et al. Regulation of histone gene transcription in yeast. *Cell Mol Life Sci*  
629 **71**, 599-613 (2014).
- 630 57. Barcaroli, D. et al. FLASH is required for histone transcription and S-phase  
631 progression. *Proc Natl Acad Sci U S A* **103**, 14808-12 (2006).
- 632 58. Chapman, R.D. et al. Transcribing RNA polymerase II is phosphorylated at CTD  
633 residue serine-7. *Science* **318**, 1780-2 (2007).
- 634 59. Schuller, R. et al. Heptad-Specific Phosphorylation of RNA Polymerase II CTD. *Mol*  
635 *Cell* **61**, 305-14 (2016).
- 636 60. Lin, A. et al. Off-target toxicity is a common mechanism of action of cancer drugs  
637 undergoing clinical trials. *Sci Transl Med* **11**(2019).
- 638

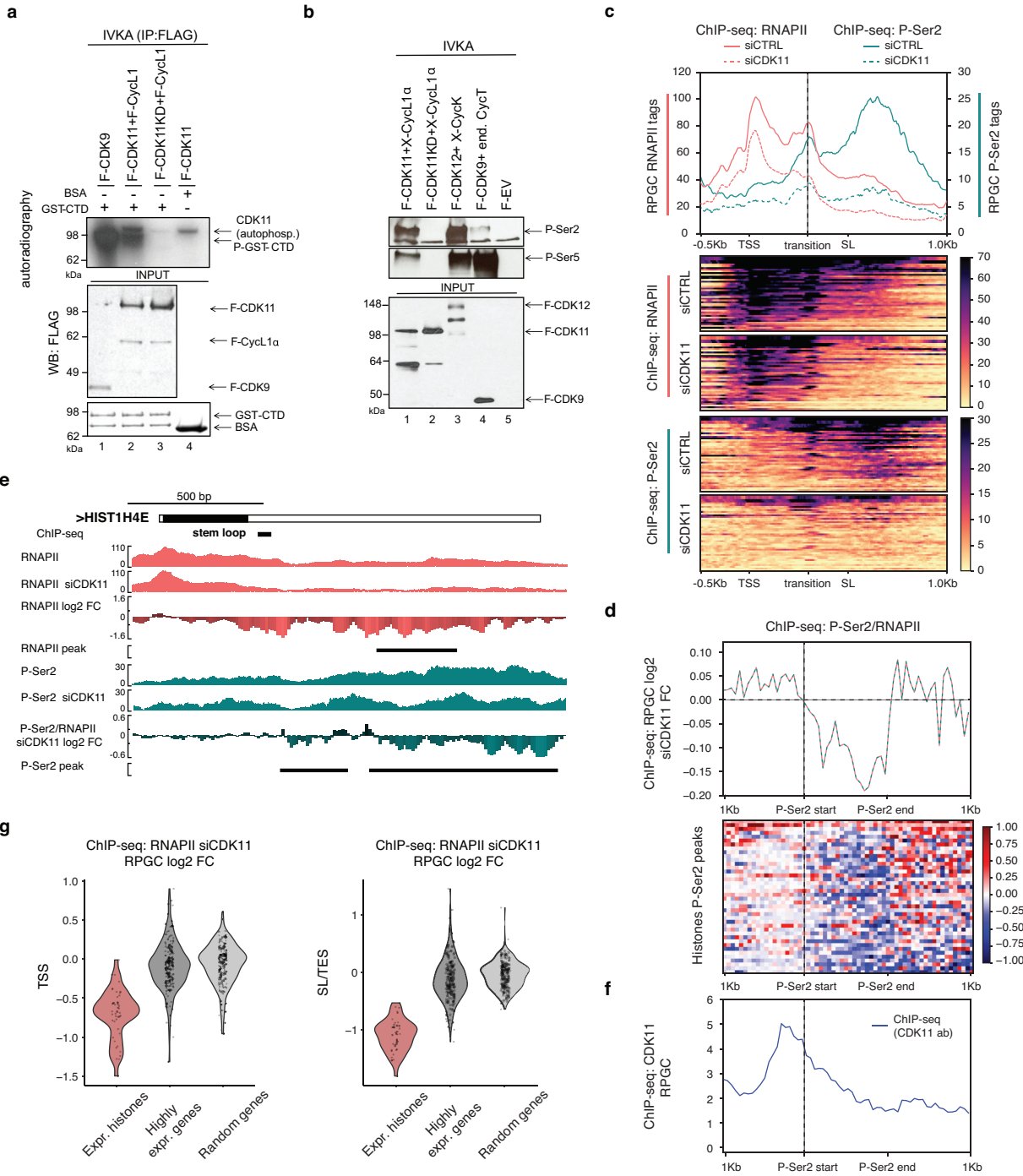
**a****b****c**

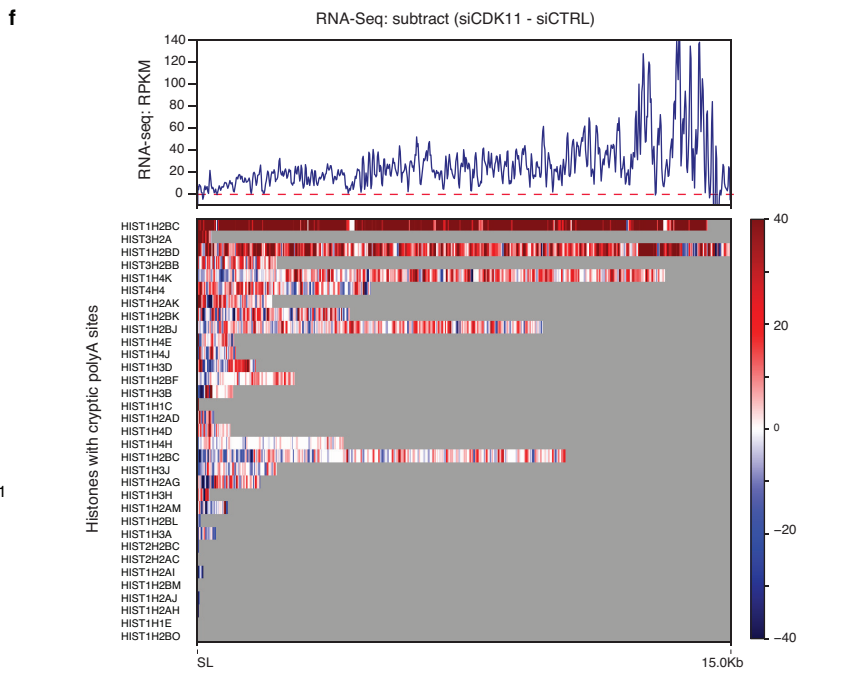
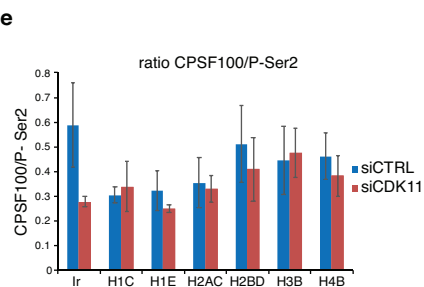
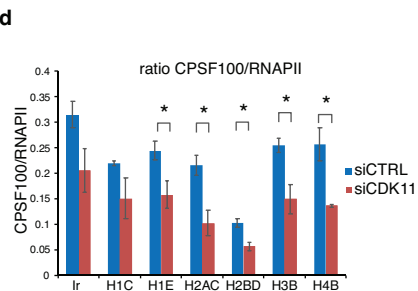
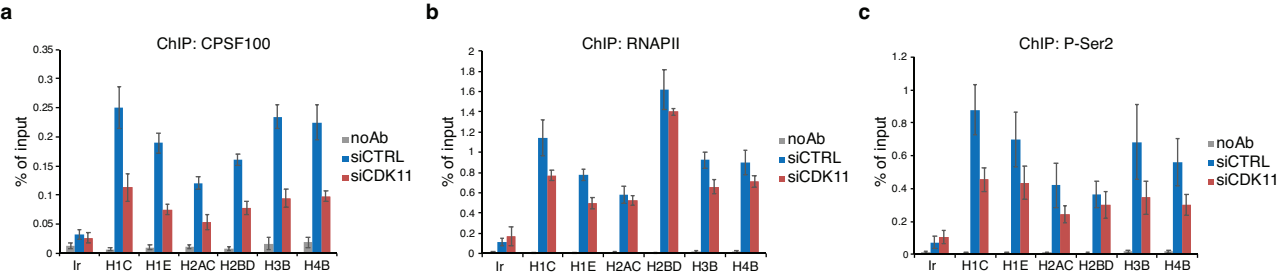


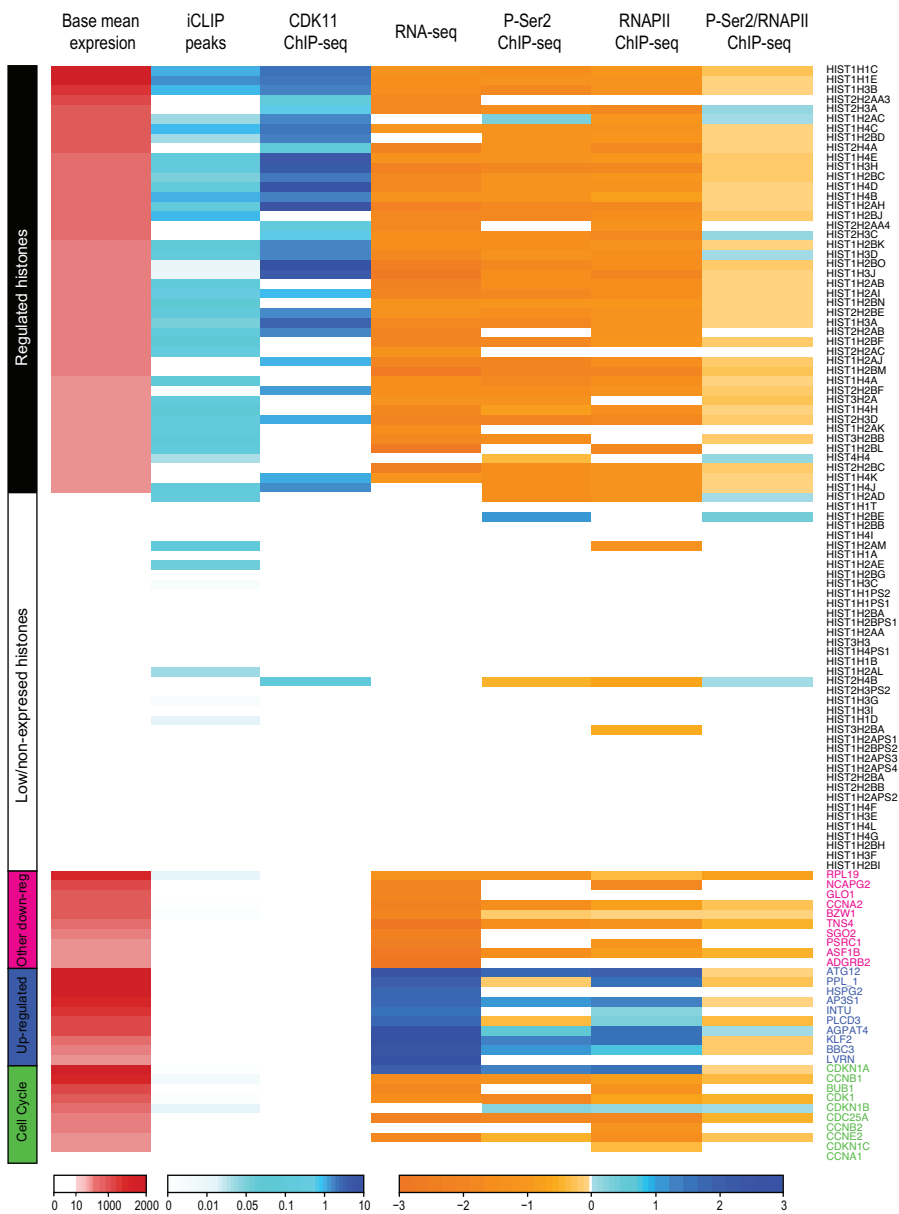
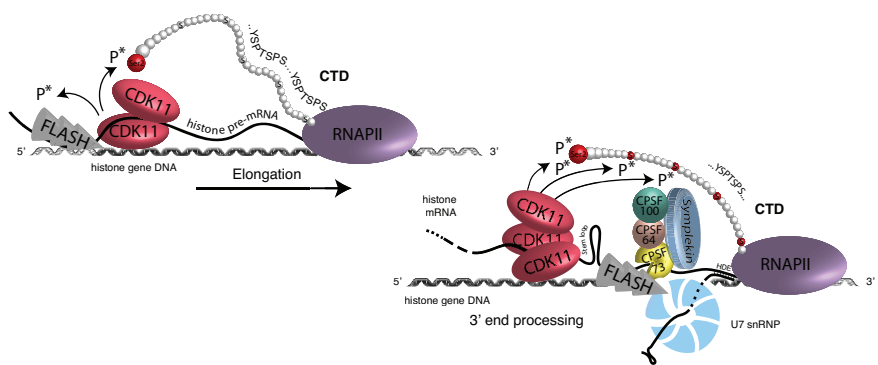
**a****b****c****d****e**

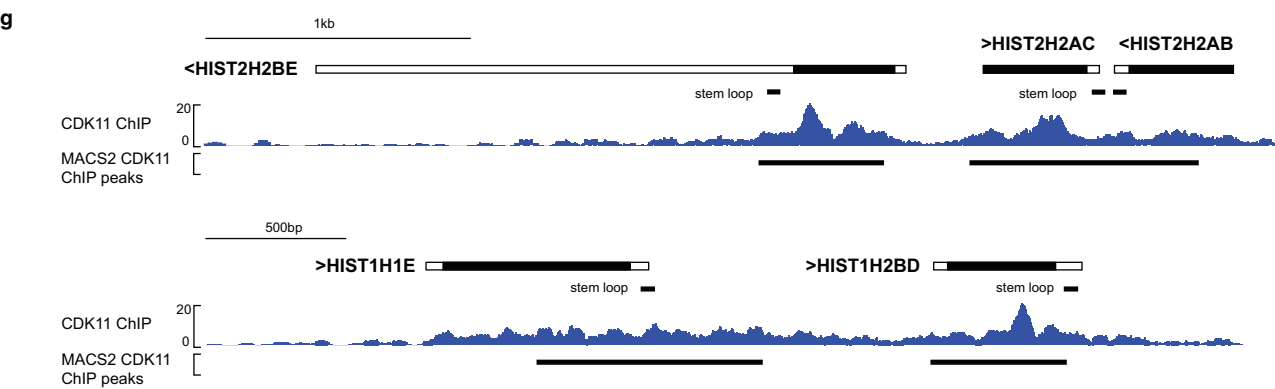
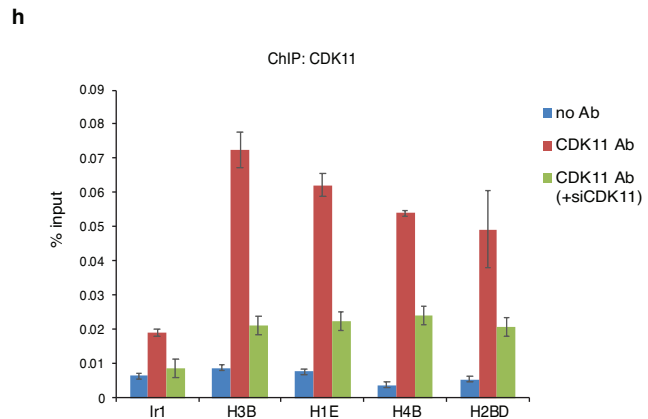
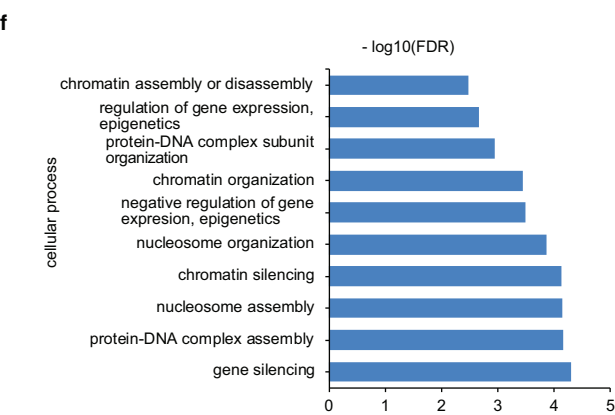
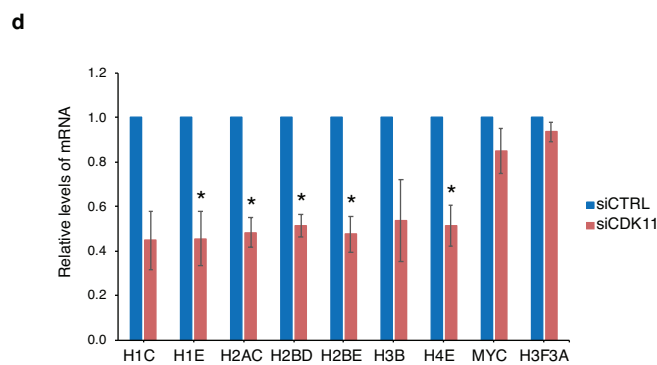
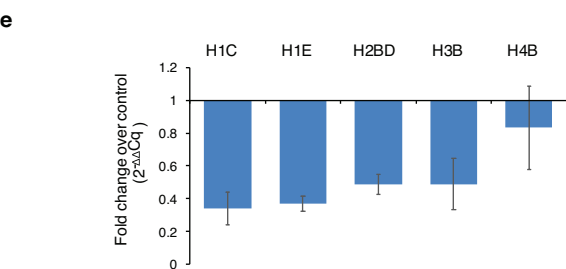
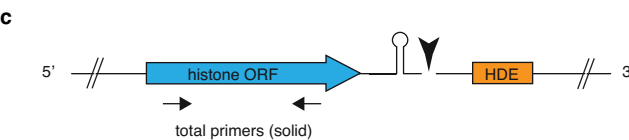
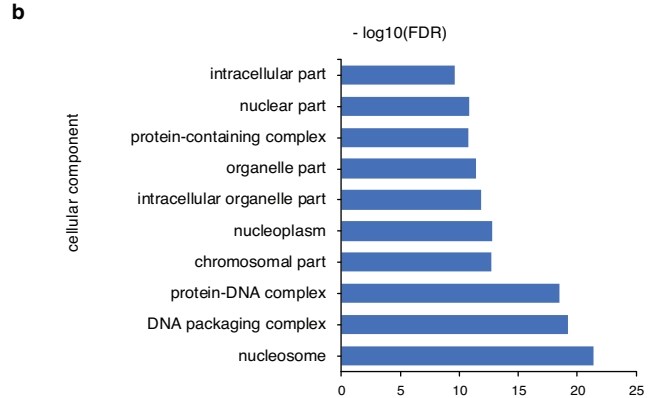
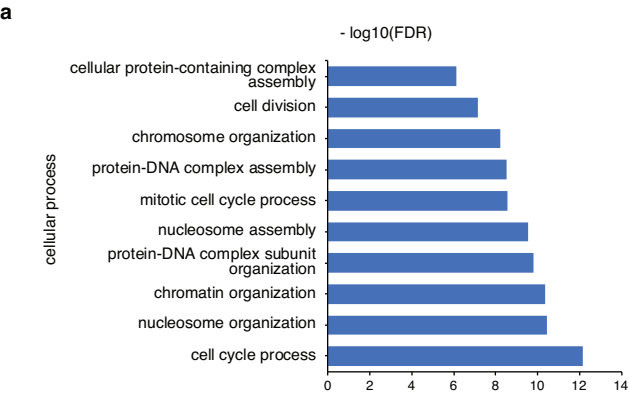


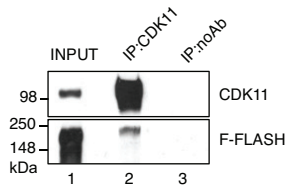
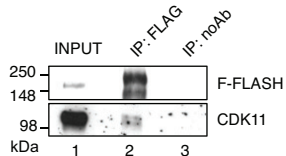
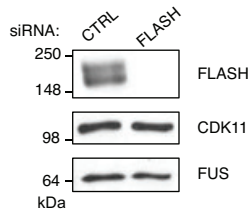
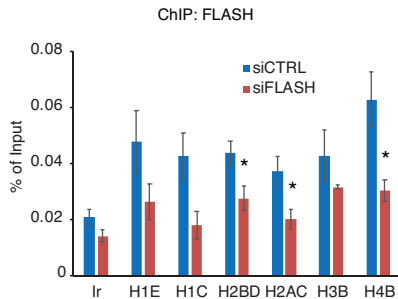
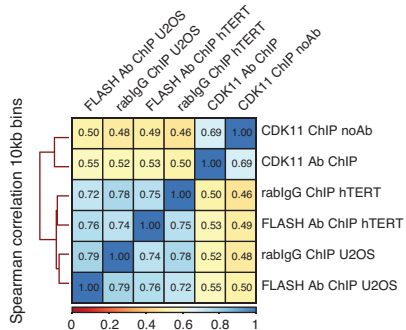




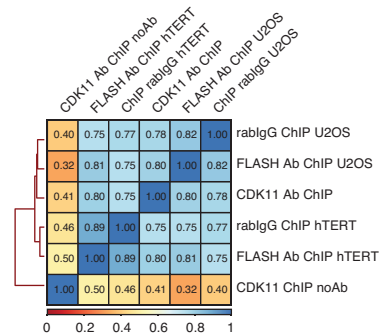


**a****b**

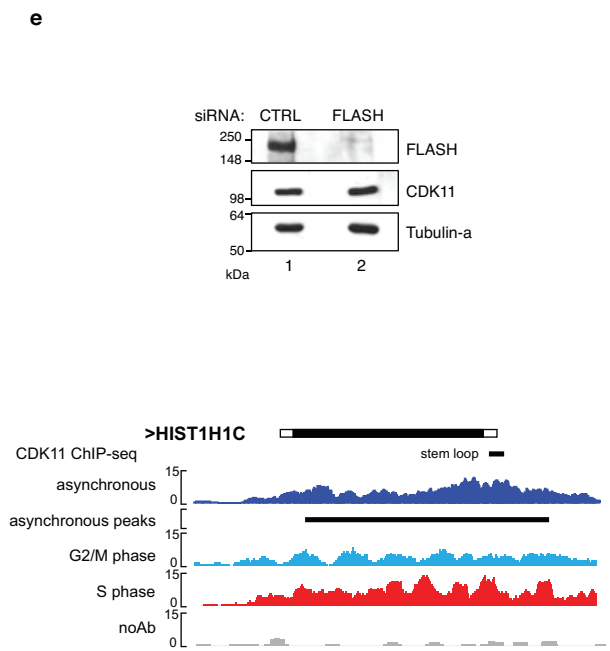
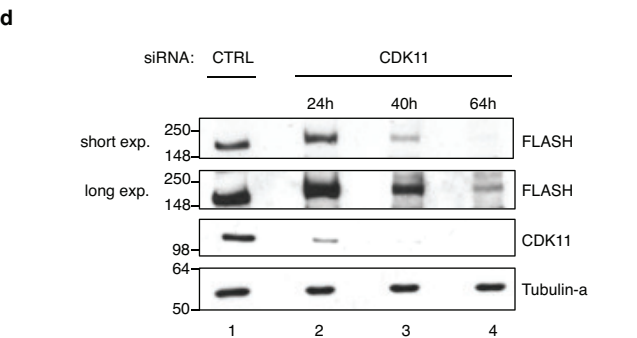
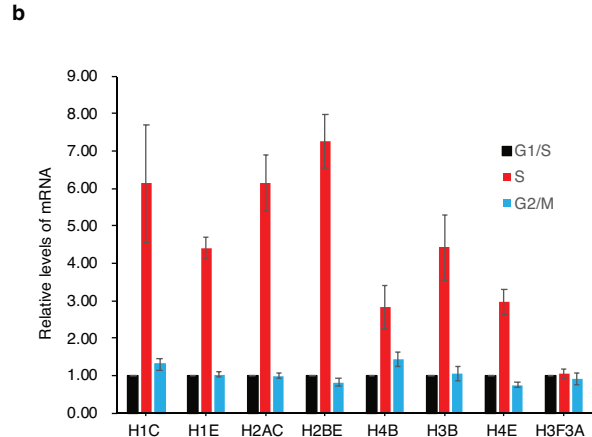
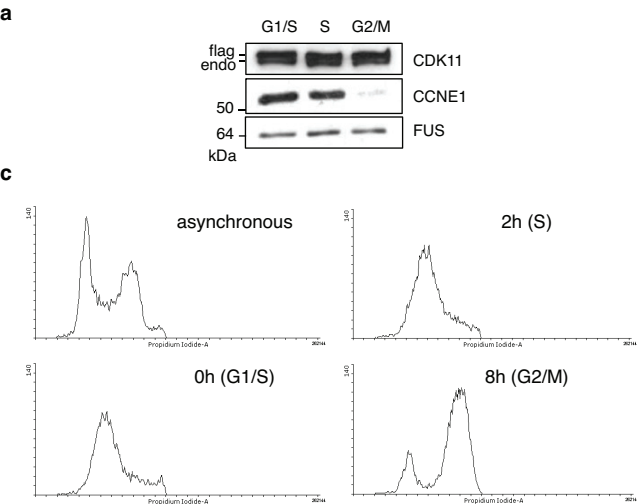


**a****b****d****e****c**

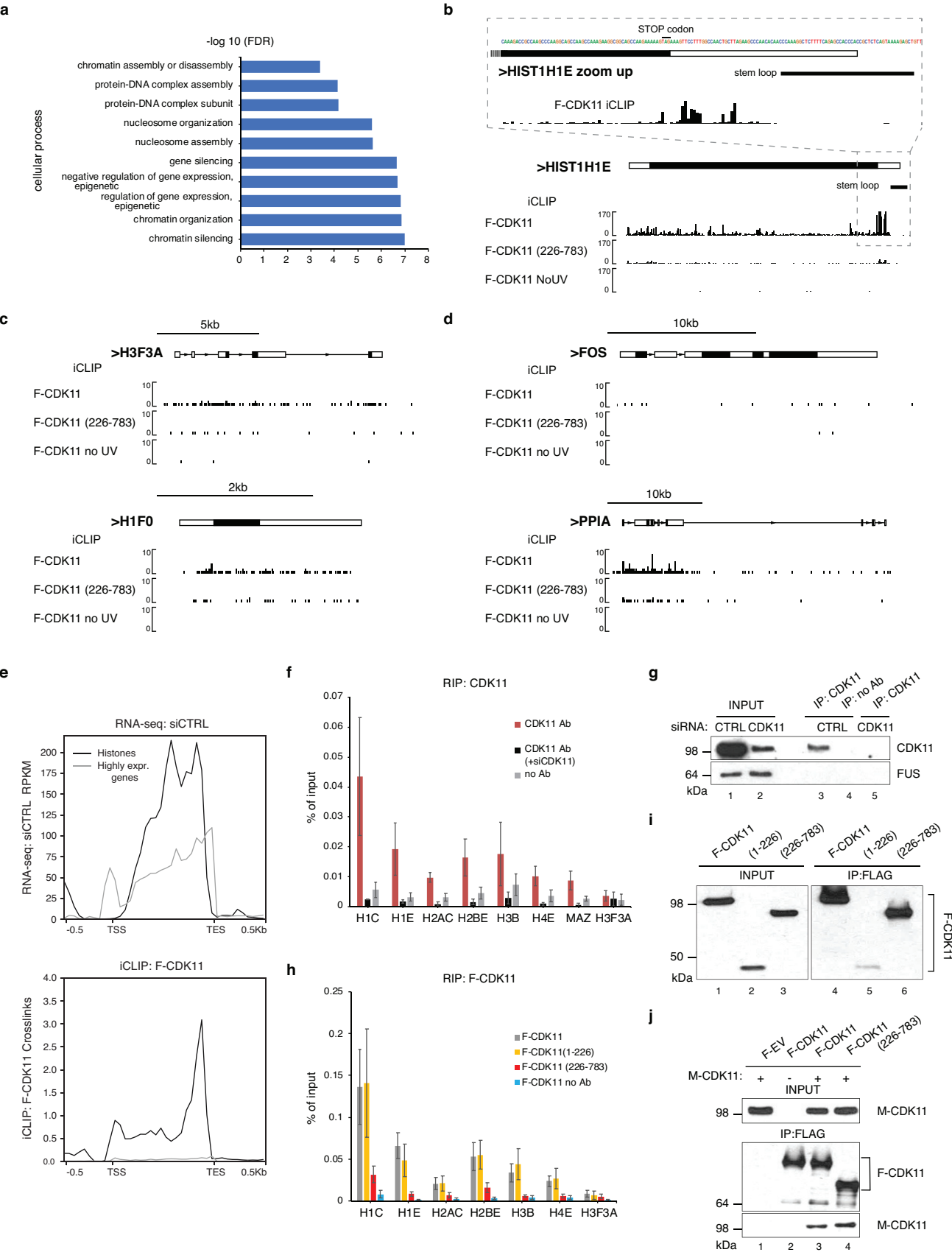
Spearman correlation on histones

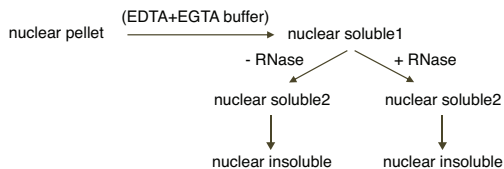
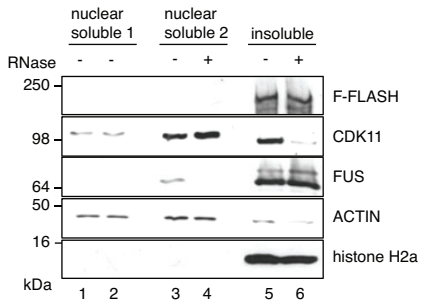
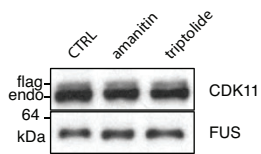
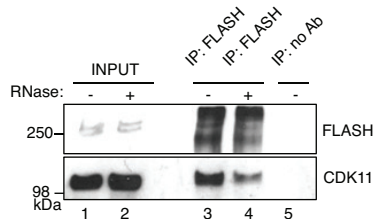










**a****c****e****b****d**